ARQII Publication
http://arqiipubl.com/ams
APPLICATIONS OF MODELLING AND SIMULATION
eISSN 2600-8084
VOL 5, 2021, 200-206

A Flexibility and Accuracy Comparison Study of Different Current-Voltage Equations for Double-Gate Nano-MOSFET by Simulation and Theory

Ooi Chek Yee* and Wong Pei Voon

Faculty of Information and Communication Technology, Universiti Tunku Abdul Rahman, Jalan Universiti, Bandar Barat, 31900 Kampar, Perak, Malaysia

*Corresponding author: ooicy@utar.edu.my

Submitted 28 October 2021, Revised 07 December 2021, Accepted 15 December 2021.

Abstract: Non-equilibrium Green's function (NEGF) is a popular method for simulation and modelling of non-equilibrium electron quantum ballistic transport in open mesoscopic system, which is double-gate (DG) nano-MOSFET in this paper, with self-energy scattering effects. In this paper, on-line device simulator nanoMOS using NEGF with finite difference method (FDM) discretization is used to obtain current-voltage (I-V) graph. The simulated on-state current is compared with the calculated and plotted using freeware Scilab code without including NEGF with FDM method to demonstrate the flexibility and accuracy of NEGF with FDM method. Accuracy of 92% is achieved. The difference in due to output resistance at saturation region of I-V curve. Also, this quantum transport model is compared with two others electron transport models derived through Boltzmann statistics along with Einstein relationship, one with high drain bias while other with traditional MOSFET model with ballistic mobility. After analysis, these two approximated equations show 0.87 and 8.8 times, respectively, matches against simulated value. Obviously, nano-MOSFET under high drain bias is closely matched with the quantum model. The traditional MOSFET with ballistic mobility is suitable for very-short-channel length devices (like DG nano-MOSFET) and III-V channel materials with very high-real mobility devices.

Keywords: Conventional model; Current-voltage; Nano-MOSFET; NEGF; Quantum transport.

1. INTRODUCTION

Currently, complementary metal-oxide-semiconductor (CMOS) technology forms the backbone of digital consumer products such as mobile phones and computers. Millions of CMOS units can be interconnected to form micro-processor unit suitable for those consumer products to do complicated arithmetic and logical operations. One major challenge of this digital technology is the drastic requirement of high-speed logic circuits within a small chip. This can be achieved by downscaling of nano-MOSFETs. Continuous downscaling of nano-MOSFET to nanometer regime has caused researchers to describe the electron transport in silicon channel by quantum mechanical features [1, 2]. This electron quantum transport has to be studied through numerical modelling of open quantum device [3, 4]. This development requires the utilization of computer simulation to investigate electrical characteristics of nano-MOSFET [5-8]. This paper emphasizes on current-voltage (I-V) curve and equations with proper electron transport models [9]. In order to exploit the high speed processing power of computer simulation, on-line device simulator nanoMOS using Non-equilibrium Green's function (NEGF) with finite difference method (FDM) discretization has been adopted [10]. The important concept of NEGF with FDM method is justified by Scilab plot without including NEGF with FDM method [11].

2. REVIEW OF THE NEGF FORMALISM AND SELF-CONSISTENT SOLUTION

Figure 1 shows the device structure and contacts which is used in nanoMOS simulation tool to produce I-V curve [12, 13]. Ω_D is the device region which includes the contacts and device. Ω_α is the area of contact α where $\alpha = 1,2,3,4$. Γ_α is defined as the boundary between Ω_α and Ω_D. Ω denotes the entire region of the device and the contacts. The above domain is summarized in Equation (1) to (3):

$$\Omega = \Omega_D \cup (\Sigma_\alpha \Omega_\alpha) = \Omega_D \cup (\Omega_1 + \Omega_2 + \Omega_3 + \Omega_4) \quad (1)$$

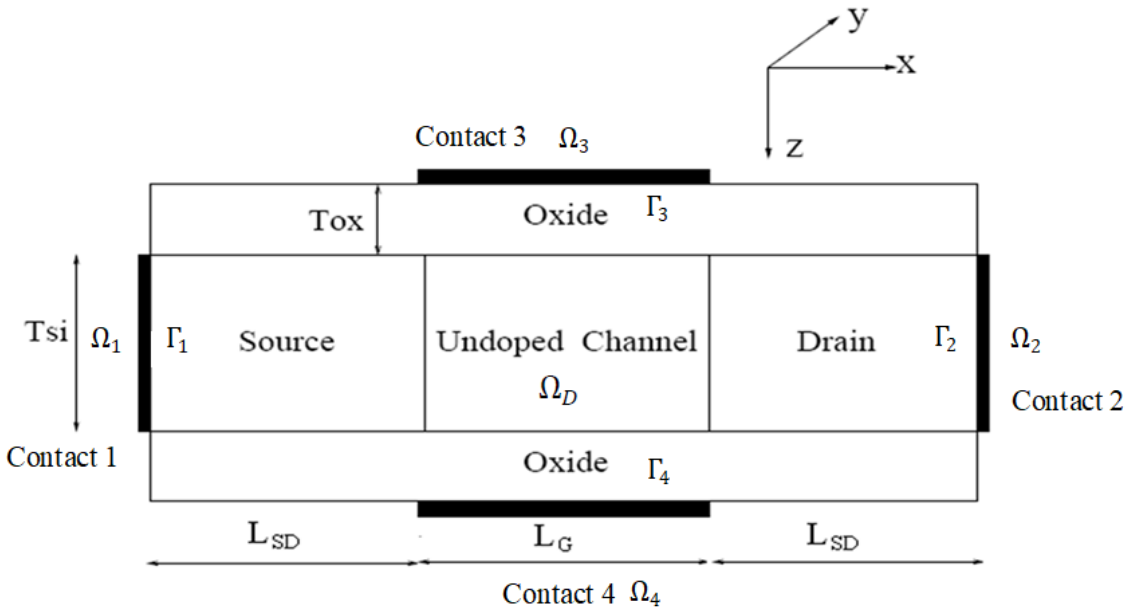

Figure 1. Structural DG nano-MOSFET used in nanoMOS simulation tool with contacts and device

Table 1. Device simulation settings of Figure 1

Double Gate nano-MOSFET Device Simulation Parameters			
V_{GS}	0.60 V	Source Length/Drain Length (L_{SD})	7.5 nm
V_{DS}	0.60 V	Silicon Channel Thickness (T_{Si})	1.5 nm
Ambient Temperature	300 K	Top/Bottom Oxide Insulator Thickness (T_{OX})	1.5 nm
V_T	0.20 V	Top/Bottom Insulator Relative Dielectric Constant	3.9
Source/Drain Doping Concentration (N_D)	$1x10^{20}$ cm^{-3}	Longitudinal Relative Electron Mass Ratio	0.98
Body Doping Concentration	0 cm^{-3}	Transverse Relative Electron Mass Ratio	0.19
Channel Length (L)	10 nm	Channel Body Relative Dielectric Constant	11.7
Source/Drain Overlap	0 nm	Top/Bottom Gate Contact Work Function	4.188 eV

$$\Gamma_0 = \Gamma_D - \Sigma_\alpha \Gamma_\alpha = \Gamma_D - (\Gamma_1 + \Gamma_2 + \Gamma_3 + \Gamma_4) \tag{2}$$

$$\Gamma_\alpha = \Gamma_D \cap \partial\Omega_\alpha \text{ with } \Gamma_D = \partial\Omega_D \tag{3}$$

Table 1 shows the device settings parameters of Figure 1 [14]. Practically, only the device domain Ω_D is used by Green's function, which is defined in Equation (4) for a certain energy E, without considering the Green's function for the rest of the exterior domain. A self-energy Σ term is included to describe the effect of contacts where the Hamiltonian H^0 is given by Equation (5).

$$(E - H^0 - \Sigma)G(\boldsymbol{r}, \boldsymbol{r}') = \delta(\boldsymbol{r} - \boldsymbol{r}'),\ \boldsymbol{r}, \boldsymbol{r}' \in \Omega_D \tag{4}$$

$$H^0 = -\frac{\hbar^2}{2}\nabla \cdot \left(\frac{1}{m(\boldsymbol{r})}\nabla\right) + V(\boldsymbol{r}) \tag{5}$$

Numerical discretization method for this Hamiltonian is FDM [15]. Ω_D is the region where actual computation is carried out. Also, $\boldsymbol{r} = (x, z)$ and $\nabla = \left(\frac{\partial}{\partial x}, \frac{\partial}{\partial z}\right)$. $m(\boldsymbol{r})$ is the effective mass of the system, $V(\boldsymbol{r})$ is the potential energy and Planck's constant is $2\pi\hbar$. The self-energy is $\Sigma = \sum_\alpha \Sigma^\alpha + \Sigma^s$ where Σ^α is the coupling between contact α and device. Meanwhile, Σ^s is the spatially distributed self-energy of scattering events (for instance electrons-impurities and electrons-phonons interaction). For ballistic transport condition, $\Sigma^s = 0$. Assumption of decoupling of self-energies between scattering events and different contacts is considered [16,17].

For a given energy E, self-energies and Green's function are solved numerically. The resulting solutions are expressed by boldface style in matrix form, that are $\boldsymbol{G}(E)$ and $\boldsymbol{\Sigma}^\alpha(E)$. As discretization of $\delta(\boldsymbol{r} - \boldsymbol{r}')$ is an identity matrix $\mathbf{I}$, Equation (4) becomes Equation (6).

$$\boldsymbol{G}(E) = (\boldsymbol{\mathcal{E}}(E) - \boldsymbol{H}^0(E) - \sum_\alpha \boldsymbol{\Sigma}^\alpha(E))^{-1} \tag{6}$$

The non-equilibrium density matrix is given by Equation (7).

$$\rho = \frac{1}{2\pi}\int_{-\infty}^{+\infty} \sum_\alpha f_{\mathrm{FD}}(E-\mu_\alpha)\boldsymbol{A}^\alpha(E)\,\mathrm{d}E \tag{7}$$

where the contact α Fermi level is μ_α and the Fermi-Dirac distribution function, f_{FD}, is denoted by Equation (8).

$$f_{\mathrm{FD}}(E-\mu_\alpha) = \left(1 + \exp\left(\frac{E-\mu_\alpha}{k_B T}\right)\right)^{-1} \tag{8}$$

with temperature T and Boltzmann constant k_B. $\boldsymbol{A}^\alpha(E)$ is the spectral function denoted as Equation (9).

$$\boldsymbol{A}^\alpha(E) = \boldsymbol{G}(E)\,\boldsymbol{\Gamma}^\alpha(E)\boldsymbol{G}^\dagger(E) \tag{9}$$

The dissipative effects of contact α is described by broadening function $\boldsymbol{\Gamma}^\alpha(E)$, which is the imaginary part of the corresponding contact, that is in Equation (10).

$$\boldsymbol{\Gamma}^\alpha(E) = i\left(\boldsymbol{\Sigma}^\alpha(E) - \left(\boldsymbol{\Sigma}^\alpha(E)\right)^\dagger\right) \tag{10}$$

All the quantities described above are used to compute experimental observables, for example current. The diagonal elements of the density matrix give the electron density $n(\boldsymbol{r})$ which depends on the potential $V(\boldsymbol{r})$ [18]. By considering the space charge effect, the potential distribution is calculated self-consistently by coupling NEGF and the Poisson equation (stated in Equation (11)).

$$-\nabla\cdot\left(\varepsilon(\boldsymbol{r})\nabla V(\boldsymbol{r})\right) = \mathrm{e}\left(-n(\boldsymbol{r}) + N_d(\boldsymbol{r})\right) \tag{11}$$

with dielectric constant $\varepsilon(\boldsymbol{r})$ and doping density $N_d(\boldsymbol{r})$ and electronic charge e. The boundary condition of $V(\boldsymbol{r})$ will be stated in Section 5.

The self-consistent iteration procedure is as follows:

- Step 1: Start with an initial potential $V(\boldsymbol{r}) = V_0$. Assume V_i is the newly calculated potential of ith iteration which is used to compute V_{i+1}.
- Step 2: Based on V_i, solve Green's function $\boldsymbol{G}(E)$ and self-energies $\boldsymbol{\Sigma}^\alpha(E)$ and then the spectral function $\mathbf{A}^\alpha(E)$ for a given energy E.
- Step 3: By integrating the density matrix ρ with respect to the energy E, electron density $n(\boldsymbol{r})$ is obtained. For this integration, Step 2 is repeated for different sampling values of E. The self-consistent convergence parameter is set to 0.001 eV in nanoMOS.
- Step 4: Obtain a new potential V_{i+1} by inserting the electron density $n(\boldsymbol{r})$ into the Poisson Equation (11).
- Step 5: If $\|V_i - V_{i+1}\| < \epsilon$ (which is Poisson convergence parameter 1x10^{-6} eV), stop the iteration procedure, otherwise repeat the procedure from Step 2.

Since the initial guess of subband energy potential is around -0.1 eV according to Schrödinger equation, the magnitude of self-consistent convergence parameter is set around 100 times smaller, which is 0.001 eV. The convergence parameters for this simulation are subband energy potential (by Schrödinger equation) and electric potential (by Poisson Equation) value. Lastly, the ballistic electron current flow from source (contact 1) to drain (contact 2) of nano-MOSFET in Figure 1 is given by Equation (12).

$$I = \frac{\mathrm{e}}{\pi\hbar}\int_{-\infty}^{+\infty} T(E)\left(f_{\mathrm{FD}}(E-\mu_1) - f_{\mathrm{FD}}(E-\mu_2)\right)\mathrm{d}E \tag{12}$$

with transmission coefficient defined by Equation (13).

$$T(E) = \mathrm{Trace}\left(\boldsymbol{\Gamma}^1(E)\boldsymbol{G}(E)\boldsymbol{\Gamma}^2(E)\boldsymbol{G}^\dagger(E)\right) \tag{13}$$

3. TWO-DIMENSIONAL NEGF WITH FDM FOR QUANTUM DEVICE

Different method of discretization for quantum device (for example finite difference method (FDM) and finite element method (FEM)) produce different forms of G and Σ^α numerically. In this paper, FDM is used. Figure 2 shows an ultra-thin MOSFET simulation strip region Ω, which consists of 3 sub-regions; source (contact 1) Ω_1, device area Ω_D and drain (contact 2) Ω_2. The horizontal node spacing a is 0.3 nm and the vertical node spacing b is 0.15 nm. The summarize of domain is stated in Equation (14).

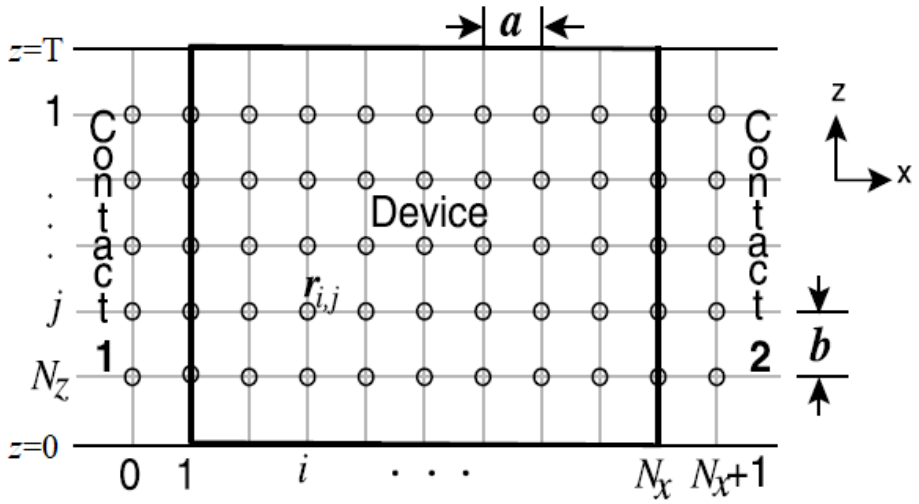

Figure 2. 2-dimensional discretization showing uniform mesh with grid spacing, a (horizontal) and b (vertical)

$$\begin{gathered}\Omega = \Omega_1 \cup \Omega_D \cup \Omega_2 \\ \Omega_1 = \{(x,z)|x \in (-\infty, x_1), z \in [0,T]\} \\ \Omega_D = \{(x,z)|x \in [x_1, x_{N_x}], z \in [0,T]\} \\ \Omega_2 = \{(x,z)|x \in (x_{N_x}, +\infty), z \in [0,T]\} \\ \Gamma_1 = \partial\Omega_1 \cap \partial\Omega_D = \{(x,z)|x = x_1, z \in [0,T]\} \\ \Gamma_2 = \partial\Omega_2 \cap \partial\Omega_D = \{(x,z)|x = x_{N_x}, z \in [0,T]\} \\ \Gamma_t = \{(x,z)|x = [-\infty, +\infty], z = T\} \\ \Gamma_b = \{(x,z)|x = [-\infty, +\infty], z = 0\}\end{gathered} \tag{14}$$

The device width (y-direction) is large so that $G(\mathbf{r}, \mathbf{r}')$ is independent of y. The two-dimensional problem specifications and notations are also listed in Figure 2. The computational domain is Ω_D. T is the silicon layer thickness, or if oxide tunneling effects is considered, the combined thickness of oxide layer and silicon layer. In this paper, electron tunneling into oxide region is ignored so that top and bottom boundaries satisfied the homogeneous Dirichlet conditions. Therefore, Equation (15) stated

$$V(\boldsymbol{r}) = \begin{cases} v^1(z) & \boldsymbol{r} \in \Omega_1 \\ v(x,z) & \boldsymbol{r} \in \Omega_D \\ v^2(z) & \boldsymbol{r} \in \Omega_2 \end{cases} \tag{15}$$

where $\boldsymbol{r} = (x,z) \in \Omega$. The relevant Green's function is denoted by Equation (16).

$$\left(E - V(\boldsymbol{r}) + \frac{\hbar^2}{2}\nabla \cdot \left(\frac{1}{m}\nabla\right)\right) G(\boldsymbol{r}, \boldsymbol{r}') = \delta(\boldsymbol{r} - \boldsymbol{r}'), \quad \boldsymbol{r}, \boldsymbol{r}' \in \Omega \tag{16}$$

with $\nabla = \left(\frac{\partial}{\partial x}, \frac{\partial}{\partial z}\right)$. Self-energies Σ^{α} (α=1,2) and Green's function are calculated by FDM which is a second-order central difference scheme.

4. CURRENT-VOLTAGE EQUATIONS FOR NANO-MOSFET

The current-voltage (I-V) equation which is simulated using nanoMOS is shown in Equation (17).

$$\frac{I_D}{W} = C_{ox}\widetilde{v_T}(V_{GS} - V_T)\left[\frac{1 - \frac{\mathcal{F}_{1/2}\left(\eta_{F1} - \frac{qV_D}{k_BT}\right)}{\mathcal{F}_{1/2}(\eta_{F1})}}{1 + \frac{\mathcal{F}_0\left(\eta_{F1} - \frac{qV_D}{k_BT}\right)}{\mathcal{F}_0(\eta_{F1})}}\right] \tag{17}$$

where C_{ox} is oxide capacitance, $\widetilde{v_T}$ is thermal velocity, η_{F1} is energy level parameter and $\mathcal{F}_j$ is Fermi-Dirac integral of order j. Equation (17) will be plotted in this paper using Scilab to show the significance of NEGF with FDM method in nano-MOSFET simulation. This equation is derived quantum mechanically as stated in [19]. This equation looks much different when compared with those equations derived using conventional MOSFET theory. However, there is an intimate relation between these two approaches. Two I-V equations modified from Equation (17) by adopting traditional MOSFET model are presented in this paper. The first equation assumes Boltzmann statistics and applies relationship between the near equilibrium

mean free path for backscattering λ_0 and the diffusion coefficient D_n, $D_n = v_T\lambda_0/2$ and Einstein relation. By this way, Equation (17) can be expressed as in Equation (18).

$$\frac{I_D}{W} = \frac{1}{L_{\text{eff}}} C_{ox}(V_{GS} - V_T)\left(\frac{1}{\mu_B} + \frac{1}{\mu_n}\right)^{-1} V_{DS} \tag{18}$$

with $\mu_n = v_T\lambda_0/(2k_BT/q)$, $\mu_B = v_T L_{\text{eff}}/(2k_BT/q)$ which is ballistic mobility and L_{eff} is the effective channel length.

Equation (18) is very suitable for very-short-channel length devices (such as DG nano-MOSFET used in this paper) or III-V materials with high real mobility [20]. The second equation is obtained under high drain bias by applying Einstein equation again. Thus, Equation (17) can be expressed as in Equation (19) with critical length of the device is l

$$\frac{I_D}{W} = C_{ox}(V_{GS} - V_T)\left[\frac{1}{v_T} + \frac{1}{(D_n/\ell)}\right]^{-1} \tag{19}$$

Equation (19) is useful for describing the electron injection velocity across low-field bottleneck at the beginning of the silicon channel. The threshold voltage in Equation (17), (18) and (19) are the same, that is 0.20 V as stated in Table 1. To determine I_D, drain to source voltage V_{DS} is set to 0.60 V and gate to source voltage V_{GS} is set to 0.60 V.

5. RESULTS AND DISCUSSION

The geometrical structure of 10 nm DG nano-MOSFET is presented in Figure 3 [21-23]. The material used in this device simulation is Silicon with wafer orientation (001)/direction [100]. Aluminium (Al) metal gate is used to set the proper gate contact work function. The dielectric insulator used is Silicon Dioxide (SiO_2). The rectangular area ABCD which comprises of oxide layer (Silicon dioxide) and silicon layer is the domain where Poisson equation is solved self-consistently with Green's function. The boundary conditions are listed in Equation (20):

$$\begin{cases} V(\boldsymbol{r}) = V_g & \boldsymbol{r} \in EF, GH \\ \frac{\partial V(\boldsymbol{r})}{\partial \boldsymbol{n}} = 0 & \boldsymbol{r} \in AB, BG, HC, CD, DF, EA \end{cases} \tag{20}$$

where the outward normal of the rectangular area is **n** and gate voltage is V_g. The direction of outward normals of the rectangular area AB, BG, HC, CD, DF and EA are **-x**, **z**, **z**, **x**, **-z** and **-z**, respectively. In this simulation setting, oxide electron tunneling is ignored. The space charge neutrality is maintained in source and drain by considering floating boundary condition, which is homogeneous Neumann condition.

Figure 4 shows the I-V curve simulated using nanoMOS with current Equation (17). Figure 5 shows the I-V curve plotted according to Equation (17) but without NEGF with FDM method. The figure shows a gradual slope in the saturation region. This slope is equivalent to output resistance of nano-MOSFET. Meanwhile, Figure 5 shows a flat line in saturation region. This is because nanoMOS uses NEGF with FDM method to compute current quantity whereas this feature is not included in the programming codes of Scilab. I_{on} in Figure 4 and Figure 5 are 2500 μA/μm and 2300 μA/μm, respectively. These two readings are 92% matched relative to 2500 μA/μm with nanoMOS is more accurate since the curve show resistance effect. The output resistance R_{out} of Figure 4 can be determined from the reciprocal of the slope in the saturation region which is 800 Ω-μm. This value is close to 900 Ω-μm as reported by Zhibin Ren [1]. Hence, it is evident that electron quantum transport model in nanodevices could be properly studied and analyzed using high speed computers which apply NEGF with FDM method.

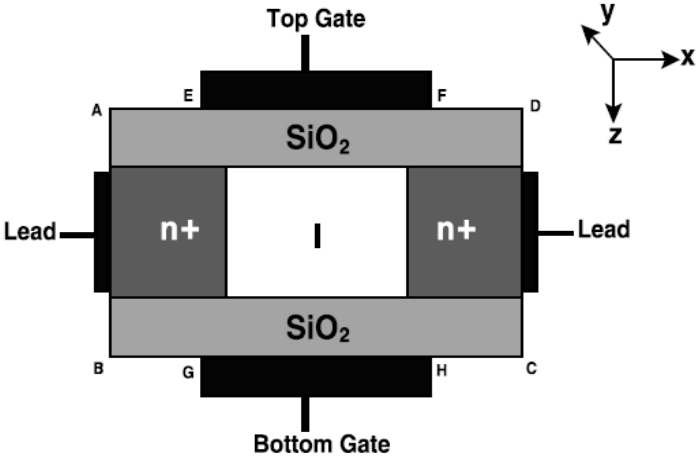

Figure 3. Geometrical structure of DG nano-MOSFET used in simulation

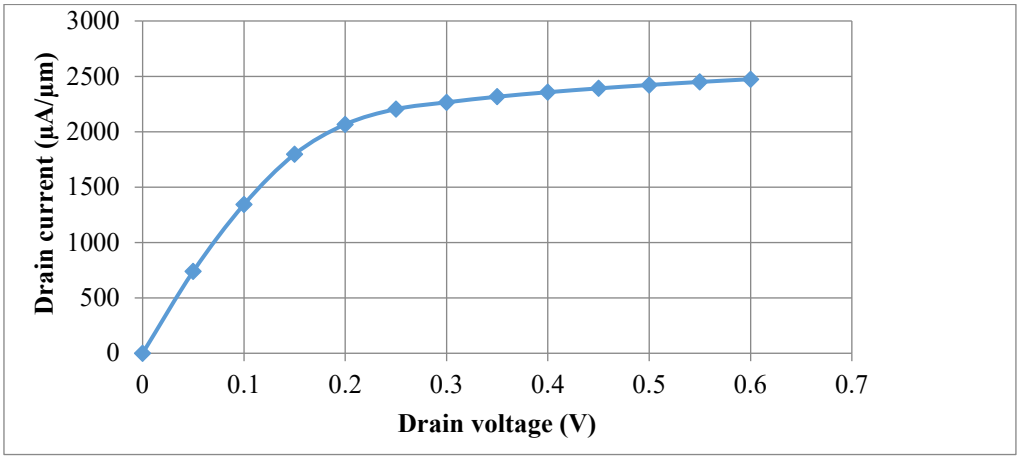

Figure 4. I-V curve simulated by nanoMOS with Green's function approach.

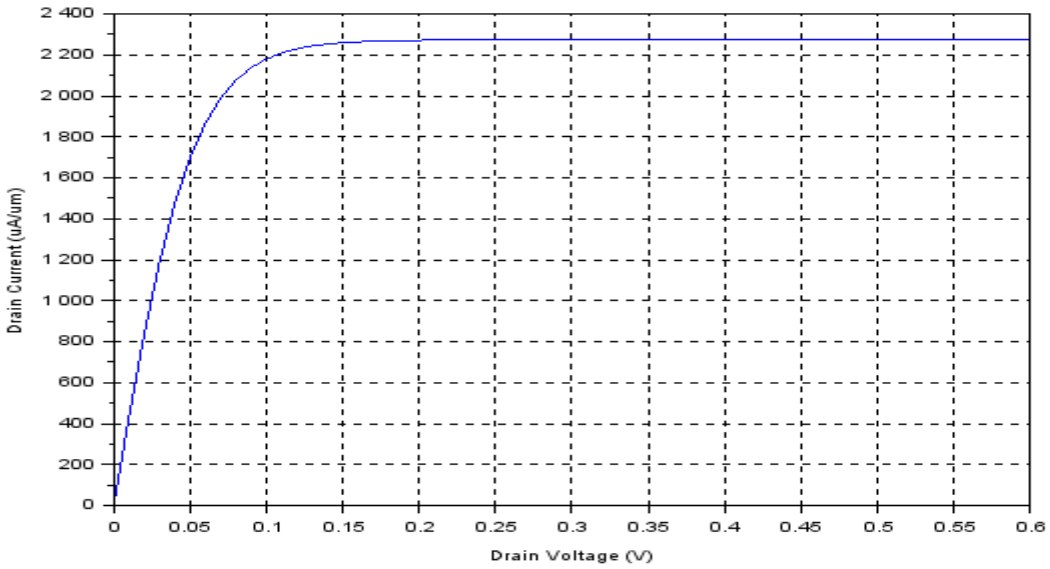

Figure 5. I-V curve plotted using Scilab without Green's function

Table 2. Benchmarking among other research works

Parameter	ITRS Target	Simulated Si (001)/[100] device	Nominal (001)/[100] device [1]	Nominal Ge (001)/[100] device [25]
I_{on} (µA/µm)	1500	2500	650	2750
R_{out} (Ω-µm)	267	800	900	145

In order to investigate the compatibility of current equation derived by quantum transport model and classical transport model, I_{on} from nanoMOS (Equation (17)) is compared with two conventional MOSFET current equations stated in Equation (18) and Equation (19). I_{on} from nanoMOS is 2500 µA/µm. I_{on} from Equation (18) is 21990 µA/µm which is 8.8 times of I_{on} from nanoMOS whereas I_{on} from Equation (19) is 2173 µA/µm which is 0.87 times of I_{on} from nanoMOS. This is because Equation (18) include ballistic mobility which is commonly found in III-V materials with very high mobility or very-short-channel nanodevices [24]. Meanwhile, Equation (19) is consistent with traditional model except that it is derived under very high drain bias and electrons diffuse across a short bottleneck at the initial part of the channel. I_{on} of nano-MOSFET is limited by this diffusion.

6. CONCLUSION

As MOSFET channel continuously to be downscaled to nanometer regime, electron transport models have been reformulated from conventional model to quantum model. The quantum model thus derived need to be investigated using computer software with includes proper methods. In this paper, NEGF with FDM method, as implemented by nanoMOS, has been verified to be a good choice in term of accuracy where quantum properties, such as current, can be captured in the simulation result. Nano-transistor device simulation without NEGF with FDM method cannot captured quantum mechanical property properly as demonstrated by Scilab plot in this paper. Also, conventional models have the shortcoming of not able to describe the quantum transport properly.

REFERENCES

[1] Z. Ren, *Nanoscale MOSFETs: Physics, simulation and design,* Ph.D. Dissertation, Purdue University, 2001.

[2] M. Baldo, *Introduction to Nanoelectronics*, MIT Open Course Ware Publication, 2011.

[3] A. E. Atamuratov, A. Yusupov, Z. A. Atamuratova, J. C. Chedjou and K. Kyamakya, Lateral capacitance-voltage method of nanoMOSFET for detecting the hot carrier injection, *Applied Sciences*, 10, 2020, 7935.

[4] I. Pappas, G. Ghibaudo, C.A. Dimitriadis and C. Fenouillet-Beranger, Backscattering coefficient and drift-diffusion mobility extraction in short channel MOS devices, *Solid-State Electronics*, 53, 2009, 54-56.

[5] Ooi Chek Yee and Lim Soo King, Study of timing characteristics of not gate transistor level circuit implemented using nano-MOSFET by analyzing sub-band potential energy profile and current-voltage characteristic of quasi-ballistic transport, *World Journal of Nano Science and Engineering,* 2016, 177-188.

[6] Ooi Chek Yee, Device-circuit level simulation study of three inputs complex logic gate designed using nano-MOSFETs, *Applications of Modelling and Simulation*, 3, 2019, 1-10.

[7] Ooi Chek Yee and Lim Soo King, Nano-MOSFETs implementation of different logic families of two inputs NAND gate transistor level circuits: A simulation study, *Jurnal Teknologi*, 79, 2017, 41-49.

[8] Ooi Chek Yee, Mok Kai Ming and Wong Pei Voon, Device and circuit level simulation study of NOR gate logic families designed using nano-MOSFETs, *Platform: A Journal of Science and Technology*, 4(1), 2021, 73-84.

[9] Ooi Chek Yee, *Device and Transistor Level Circuit Performance Analysis of Nanoscale MOSFET*, Ph.D. Thesis, Universiti Tunku Abdul Rahman, 2019.

[10] Ooi Chek Yee and Lim Soo King, Simulation Study on different logic families of NOT gate transistor level circuits implemented using nano-MOSFETs, *Journal of Telecommunication, Electronic and Computer Engineering*, 8, 2016, 61-67.

[11] Ooi Chek Yee and Lim Soo King, A comparative study of quantum gates and classical logic gates implemented using solid-state double-gate nano-MOSFETs, *International Journal of Nanoelectronics and Materials,* 9, 2016, 123-132.

[12] A. V. Pawar, S. S. Kanapally, A. P. Chougule, P. P. Waifalkar, K. V. More, R. K. Kamat and T. D. Dongale, Simulation study of field-effect transistor based cylindrical silicon nanowire biosensor: Effect of length and radius of the nanowire, 11(1), 2019, 01005.

[13] V. P. Georgiev, M. M. Mirza, A. -I. Dochioiu, F. Adamu-Lema, S. M. Amoroso, E. Towie, C. Riddet, D. A. MacLaren, A. Asenov and D. J. Paul, Experimental and simulation study of silicon nanowire transistors using heavily doped channels, *IEEE Transactions on Nanotechnology,* 16(5), 2017, 727-735.

[14] R. Chakraborty and J. K. Mandal, Design of 4 nm MOSFET and its applications, *Microsystem Technologies*, 2018, 1-8.

[15] X. Wang, *NanoMOS 4.0: A Tool to Explore Ultimate Si Transistors and Beyond,* Master of Science Thesis, Purdue University, 2010.

[16] U. Wulf, M. Krahlisch and H. Richter, Scaling properties of ballistic nano-transistors, *Nanoscale Research Letters*, 6, 2011, 1-8.

[17] P. A. G. Sankar and K. Udhayakumar, MOSFET-like CNFET based logic gate library for low-power application: A comparative study, *Journal of Semiconductors*, 35(7), 2014, 075001.

[18] H. Jiang, S. Shao, W. Cai and P. Zhang, Boundary treatments in non-equilibrium Green's function (NEGF) methods for quantum transport in nano-MOSFETs, *Journal of Computational Physics*, 227, 2008, 6553-6573.

[19] M. Lundstrom, Notes on the Ballistic MOSFET, *Network for Computational Nanotechnology*, Purdue University, 2005.

[20] C. Jeong, D. A. Antoniadis and M. S. Lundstrom, On backscattering and mobility in nanoscale silicon MOSFETs, *IEEE Transactions on Electronic Devices*, 56(11), 2009, 2762-2769.

[21] A. Ziabari, M. Charmi and H. R. Mashayekhi, The impact of body doping concentration on the performance of nano DG-MOSFETs: A quantum simulation, *Chinese Journal of Physics*, 51(4), 2013, 844-853.

[22] M. L. P. Tan, G. Lentaris and G. AJ Amaratunga, Device and circuit-level performance of carbon nanotube field-effect transistor with benchmarking against a nano-MOSFET, *Nanoscale Research Letters*, 7, 2012, 1-10.

[23] H. C. Chin, C. S. Lim, W. S. Wong, K. A. Danapalasingam, V. K. Arora and M. L. P. Tan, Enhanced device and circuit-level performance benchmarking of graphene nanoribbon field-effect transistor against a nano-MOSFET with interconnects, *Journal of Nanomaterials*, 2014, 1-14.

[24] A. Islam and K. Kalna, Analysis of electron transport in the nano-scaled Si, SOI and III-V MOSFETs: Si/SiO_2 interface charges and quantum mechanical effects, *The 2nd International Workshop on Materials Science and Mechanical Engineering*, Bristol, UK, 504, 2019, 012021.

[25] A. Rahman, *Exploring New Channel Materials for Nanoscale CMOS Devices: A Simulation Approach*, Ph.D. Dissertation, Purdue University, 2005.